

# Molecular Dynamics of C<sub>70</sub>S<sub>48</sub>: Dielectric Function and NMR Study

A. V. Talyzin\*

Ångström Laboratory, Inorganic Chemistry, Box 538, SE-751 21 Uppsala, Sweden

A.-S. Grell† and F. Masin

Universite Libre de Bruxelles, CP-232, Bd. Du Triomphe, B-1050 Bruxelles, Belgium

A. B. Sherman and V. V. Lemanov

A.F. Ioffe Physico-Technical Institute, RAS, Politechnic strasse 26, 194021 St. Petersburg, Russia

P. Lunkenheimer, R. Brand, and A. Loidl

Universität Augsburg, Experimentalphysik V, Universitätsstrasse 2, 86135 Augsburg, Germany

Received: October 12, 2000

Molecular dynamics of C<sub>70</sub>S<sub>48</sub> have been studied by dielectric relaxation spectroscopy and NMR. In accordance with the NMR data, the rotation of C<sub>70</sub> molecules is not hindered by sulfur, and even at room temperature, it is uniaxial like that in pure C<sub>70</sub>. Numerous phase transitions observed for pure C<sub>70</sub> have no analogues in C<sub>70</sub>S<sub>48</sub>. The only anomaly of the dielectric function was found at 245 K. In accordance with the NMR data, C<sub>70</sub> molecules rotate uniaxially at room temperature, but below 170 K, this rotation begins to freeze, and at 150 K, the rotation is frozen in the NMR scale. Dielectric function temperature dependence does not show any anomalies around 170 K, where the NMR registered a freezing of the rotational freedom of C<sub>70</sub> molecules, and the NMR does not show any features around 245 K, where the dielectric function shows a sharp anomaly. Some possible explanations for the nature of the anomaly around 245 K are discussed.

## 1. Introduction

The sulfur–C<sub>70</sub> compounds are relatively less investigated compared to other groups of fullerene materials. The family of sulfur–fullerene compounds now includes C<sub>60</sub>S<sub>16</sub>,<sup>1</sup> C<sub>60</sub>(CS<sub>2</sub>)S<sub>16</sub>,<sup>2</sup> C<sub>70</sub>S<sub>48</sub>,<sup>3,4</sup> C<sub>70</sub>S<sub>8</sub>,<sup>5</sup> and C<sub>76</sub>S<sub>48</sub>.<sup>6</sup> All of these materials have similar structures: the main structural elements are fullerene molecules connected by weak van der Waals bonds with crown-shaped S<sub>8</sub> rings. Usually, crystals of all of these materials have been grown from a solution of fullerene and sulfur in CS<sub>2</sub>. An alternative method of a reaction of C<sub>60</sub> (or other fullerenes) with a sulfur melt gives only polycrystalline samples.<sup>3</sup>

Apart from crystal structures, there are only very few data available about other properties of these compounds. Anomalous optical absorption of C<sub>70</sub>S<sub>48</sub> has been noted already in the first report about this material (Roth and Adelman<sup>1</sup>). Recently, investigations of optical properties of C<sub>70</sub>S<sub>48</sub> were published by Semkin et al.<sup>7</sup> Furthermore, methods for the preparation of thin films of C<sub>70</sub>S<sub>48</sub> and C<sub>60</sub>S<sub>16</sub> have been reported,<sup>8</sup> as well as crystallization experiments which were allowed to grow large C<sub>70</sub>S<sub>48</sub> crystals.<sup>9</sup>

The structure of C<sub>70</sub>S<sub>48</sub> was solved by Roth and Adelman<sup>3</sup> and Bürgi et al.<sup>4</sup> The structure is orthorhombic (space group *Amm*2: *a* = 37.953, *b* = 20.241, and *c* = 10.226 Å), which makes C<sub>70</sub>S<sub>48</sub> especially interesting for dielectric measurements, because this space group is pyroelectric and characterized by a spontaneous polarization as an inherent element of the structure. Preliminary data of DRS (dielectric relaxation spectroscopy) were reported recently by Sherman et al., revealing an anomaly

around 245 K.<sup>10</sup> The nature of this anomaly cannot be identified from dielectric properties alone, and other methods are required to provide additional information.

An interesting question is, what is the rotational state of sulfur fullerenes? The structures of C<sub>70</sub>S<sub>48</sub> and C<sub>60</sub>S<sub>16</sub> were solved by X-ray diffraction, yielding fixed positions of each carbon atom, a fact that suggests that the fullerene molecules are fixed concerning the orientational degrees of freedom.<sup>1,3,4</sup> However, the Raman and IR studies reveal that the spectra of these compounds are almost identical compared to the spectra of pure C<sub>70</sub> and C<sub>60</sub>.<sup>7</sup> Only slight differences because of bonding between fullerenes and sulfur rings were observed. These spectra suggest that fullerenes molecules in C<sub>70</sub>S<sub>48</sub> and C<sub>60</sub>S<sub>16</sub> undergo a rotational motion similar to the room-temperature phases of C<sub>60</sub> and C<sub>70</sub>. These conclusions have been proven by recent NMR results on the molecular dynamics of C<sub>60</sub>S<sub>16</sub>.<sup>11</sup> This study showed that C<sub>60</sub> molecules in C<sub>60</sub>S<sub>16</sub> undergo fast reorientational motion and detected a steep change of this motion at 150 K. With a similar bonding in C<sub>70</sub>S<sub>48</sub> and C<sub>60</sub>S<sub>16</sub> taken into account, it is possible to suggest similar rotational dynamics of the fullerene molecules in these two compounds. Here we present a study of the dielectric properties of C<sub>70</sub>S<sub>48</sub>, combined with results obtained by NMR.

## 2. Experimental Section

Crystallization experiments were performed with C<sub>70</sub> of 99% purity (MER Corp.) and sulfur of 99.999% purity. Crystals were grown by slow evaporation of a benzene solution of C<sub>70</sub> and sulfur. A sulfur concentration, several times higher compared to the stoichiometry C<sub>70</sub>S<sub>48</sub>, was used to avoid the formation of C<sub>70</sub>S<sub>8</sub> phase.<sup>5</sup> Crystals of C<sub>70</sub>S<sub>48</sub> usually are red transparent flat

\* To whom correspondence should be addressed.

† FRIA Grant holder.

needles with (100) main faces and a size up to  $10 \times 1 \times 0.1$  mm. The 2-fold axis is directed in the plane of the platelet at  $45^\circ$  with regard to the long direction of the needle. The direction of the polar axis was defined according to the effect of anomalous light absorption.<sup>3</sup> In most cases, our samples were not perfect single crystals. They consisted of many small sheets with slightly different orientation. The powder diffraction data were recorded at room temperature. The cell parameters for C<sub>70</sub>S<sub>48</sub> are  $a = 38.23$ ,  $b = 20.46$ , and  $c = 10.34$  Å, which is in good agreement with the published data.<sup>3,4</sup>

Thin films of C<sub>70</sub>S<sub>48</sub> were obtained by two different methods. In both methods, C<sub>70</sub> films were predeposited onto substrates and subjected to a reaction with sulfur. In the first method, the C<sub>70</sub> film reacted with sulfur in a saturated sulfur solution in toluene. In the second method, the reaction was conducted with a saturated sulfur vapor in a sealed ampule. The detailed study of C<sub>70</sub>S<sub>48</sub> thin-film growth and its properties were reported recently by Talyzin and Jansson.<sup>8</sup> X-ray-diffraction analysis showed that the films synthesized by both methods consisted only from single phase C<sub>70</sub>S<sub>48</sub> and that all of the C<sub>70</sub>S<sub>48</sub> films exhibited a preferential (100) orientation.

Real and imaginary parts of the complex dielectric constant  $\epsilon^* = \epsilon' - i\epsilon''$  were recorded in the frequency range 20 Hz to 1 MHz, using the autobalance bridge HP4284A. To carry out measurements as a function of temperature, the samples were mounted in a helium refrigerator system in a vacuum chamber. Electrodes for dielectric measurements were painted on the main faces of the crystals with silver paint. When thin films were studied, coplanar gold electrodes were prepared by evaporation.

To observe special features of polarization behavior, the temperature dependence of the dielectric constant along the polar axis should be measured. Unfortunately, such measurements in our needlelike platelet crystals are practically impossible because of a specific platelet shape, with the polar axis being aligned in the plane of the platelet at  $45^\circ$  to the needle direction. We were able to make measurements of the complex dielectric constant only in the direction perpendicular to the (100) face. However, we believe that because of a small misorientation of a different part of the sample (as noted before) there is a small contribution of the dielectric constant component along the polar [001] axis.

For thin films, the situation is different. Even simple observations under an optical microscope showed that the crystallites in these films also have the shape of flat platelets, which are preferentially oriented with the (100) face parallel to the substrate. In the plane of the films, crystallites are oriented randomly. Because we used coplanar electrode geometry on the films, the dielectric constant components along the [001] polar axis were detected.

The <sup>13</sup>C NMR measurements were performed by means of a Bruker MSL 300 spectrometer and a superconducting coil, delivering a 7.05 T magnetic field (working frequency for <sup>13</sup>C: 75.47 MHz). All chemical shifts are given with respect to the <sup>13</sup>C resonance frequency in tetramethylsilane. The <sup>13</sup>C (in natural abundance) spin–lattice relaxation time,  $T_1$ , was obtained by using a saturation–recovery pulse sequence. The sample (inside a 4 mm diameter rotor) was located in a Bruker low-temperature probe (4–500 K), and the temperature was varied by means of an Oxford CF1200 cryostat. Magic angle spinning (MAS) experiments were run with a 4 mm Bruker MAS probe, and the rotating working frequencies were 5 kHz and 1285 Hz. MAS simulation spectra were made using Bruker software.

### 3. Results

**3.1. Dielectric Function Measurements.** Below 100 K, the complex dielectric function  $\epsilon^*$  has a weak temperature depen-

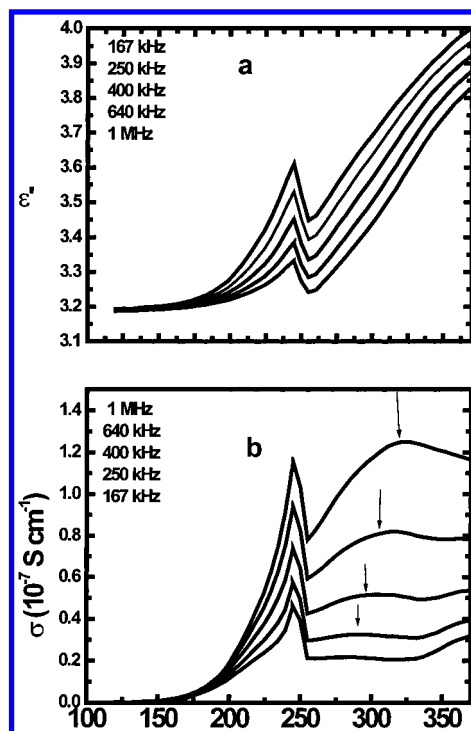


**Figure 1.** Temperature dependence of the real part of dielectric constant  $\epsilon'$  and the conductivity  $\sigma$  for various frequencies. The frequencies are (from top to bottom) (a) 167, 250, 400, and 640 kHz and 1 MHz and (b) 1 MHz and 640, 400, 250, and 167 kHz.

dence and exhibits no anomalies. This behavior has been found for all samples and for all frequencies. On the contrary, there is a rather strong nonmonotonic temperature dependence of  $\epsilon^*$  for the 100–350 K interval. The typical dependences of  $\epsilon'$  and conductivity  $\sigma$  (related to the dielectric loss by  $\sigma = \epsilon''\epsilon_0\omega$ , where  $\epsilon_0$  is the permittivity of free space) for single crystals during a heating run are shown in Figure 1. Distinct maxima of the dielectric constant and conductivity with frequency-independent temperature position at 245 K are seen. It should be noted that this anomaly was not observed during a cooling run; i.e., there is a large dependence of the dielectric response related to this anomaly on thermal history.

As can be seen in Figure 1, the maximum of the  $\epsilon'$  dependence increases with lower frequencies while the  $\sigma$  maxima decrease. Other important features in experimental dependences of  $\epsilon'$  and  $\sigma$  are the well-defined relaxation processes, which can be distinguished both above 245 K (Figure 1) and below this temperature (Figure 2). The data represent the same sample but in another frequency range. Unlike the 245 K anomaly, both relaxation processes are characterized by a frequency dependence: as the frequency increases, the anomalies move to higher temperatures. This behavior can be described by a Debye relaxation response:

$$\epsilon' = \epsilon_\infty + (\epsilon_s - \epsilon_\infty)/[1 + (\omega\tau)^2]$$

$$\epsilon'' = (\epsilon_s - \epsilon_\infty)\omega\tau/[1 + (\omega\tau)^2] \quad (1)$$

where  $\epsilon_s$  and  $\epsilon_\infty$  are the static and the high-frequency dielectric constants, respectively, and the relaxation time  $\tau$  is given by an Arrhenius law:

$$\tau = \tau_0 \exp(U/k_B T) \quad (2)$$

Fitting the experimental data (Figures 1 and 2) to eqs 1 and 2 yields an activation energy  $U_{HT} = 0.35$  eV and a relaxation

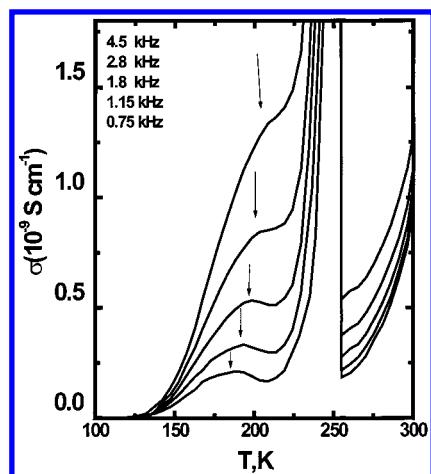


**Figure 2.** Temperature dependence of the conductivity  $\sigma$  of the same sample as in Figure 1 but in the lower frequency range. The frequencies are (from top to bottom) 4.5, 2.8, 1.8, 1.15, and 0.75 kHz.

time  $\tau_{\text{OHT}} = 7.1 \times 10^{-13}$  s for the high-temperature ( $T > 245$  K) relaxation and  $U_{\text{LT}} = 0.2$  eV and  $\tau_{\text{OLT}} = 8.4 \times 10^{-10}$  s for the low-temperature ( $T < 245$  K) relaxation. Typically, all of the films grown by the vapor method behave similarly to the sample shown in Figures 1 and 2. At the same time, the films grown by the solution method show different properties depending on crystallization conditions similar to the case of the single crystals.

**3.2.  $^{13}\text{C}$  NMR Measurements.** **3.2.1.  $^{13}\text{C}$  NMR Spectra.** At room temperature (293 K), the one-dimensional  $^{13}\text{C}$  MAS spectrum of  $\text{C}_{70}\text{S}_{48}$  (see Figure 3a) is the same as that observed for solid  $\text{C}_{70}$ ,<sup>12</sup> but the line widths ( $0.40 \pm 0.05$  ppm) are similar to  $\text{C}_{70}$  lines observed above 323 K. For comparison, the line widths for pure  $\text{C}_{70}$  are equal to 0.3 ppm in the face-centered cubic (fcc) phase ( $> 323$  K), 0.7 ppm in the rhombohedral phase ( $< 323$  K), and 0.8–1.5 ppm (the lines broadened) below 273 K.

In this figure, all resonance lines are centerbands because we used fast MAS ( $\nu_r = 5$  kHz) measurements. These centerbands represent isotropic chemical shifts. It is also important to know that the broadening can be attributed to the anisotropic magnetic susceptibility of the  $\text{C}_{70}$  molecules.<sup>12</sup> In our case, because we do not observe a significant line broadening (no susceptibility broadening) compared to that in fcc  $\text{C}_{70}$ , directions of the long axis of the  $\text{C}_{70}$  molecules (usually designated as the  $\hat{n}$  direction) are isotropically distributed, and the bulk susceptibility must be, therefore, isotropic.

We have observed a small chemical shift of  $1.4 \pm 0.2$  ppm, compared with line positions obtained on  $\text{C}_{70}$  in solution<sup>13</sup> and  $1.7 \pm 0.2$  ppm compared with solid  $\text{C}_{70}$ .<sup>12</sup> This small shift compared to pure  $\text{C}_{70}$  does not imply Knight shift. It is reasonable to assume that this compound can be characterized essentially as a neutral van der Waals complex, and this shift is a sign that the apparent magnetic field for the  $^{13}\text{C}$  nuclei of  $\text{C}_{70}\text{S}_{48}$  is higher than for solid  $\text{C}_{70}$  (weak paramagnetism). In most other  $\text{C}_{60}$  solvates, like  $\text{C}_{60} \cdot 4\text{C}_6\text{H}_6$ , the shift is in the opposite side,  $-0.5$  ppm (weak diamagnetism).<sup>14,15</sup>

Figure 3b shows a one-dimensional  $^{13}\text{C}$  MAS spectrum at room temperature (293 K) taken under slow-spinning conditions ( $\nu_r = 1285$  Hz). In addition to the centerbands seen on the spectrum at 5 kHz, spinning sideband lines appear separated from the centerbands by a multiple of  $\nu_r$ . The simulation of this spectrum detects only three systems of lines centered to carbon sites C1, C2 and C3, and C4. The C5 system is included in the double system C2 and C3. By one-dimensional measure-

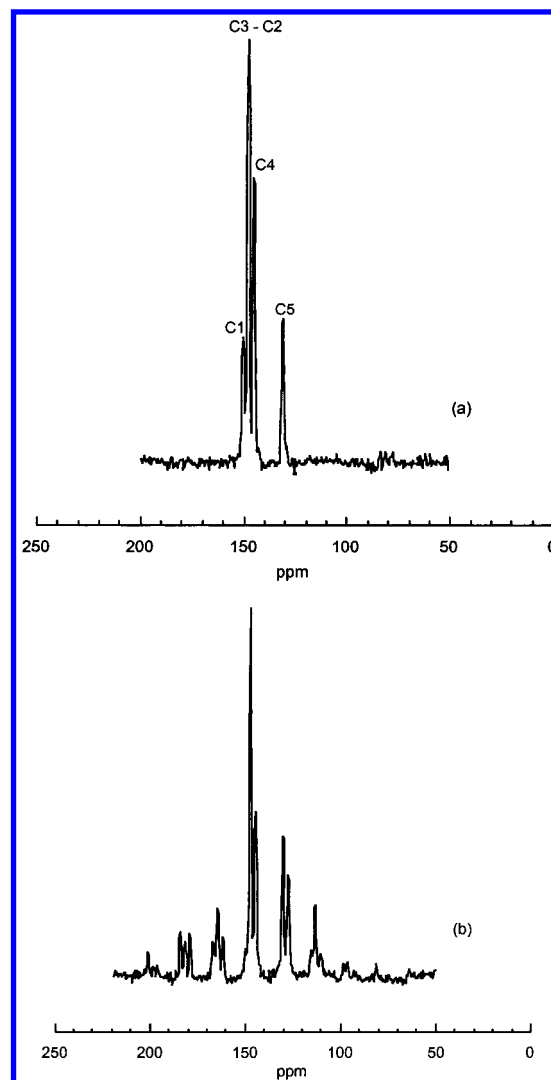


**Figure 3.**  $^{13}\text{C}$  MAS spectra of  $\text{C}_{70}\text{S}_{48}$  at room temperature. One-dimensional  $^{13}\text{C}$  MAS spectrum at 5 kHz (a) and one-dimensional  $^{13}\text{C}$  slow MAS spectrum at 1285 Hz (b).

**TABLE 1: Comparison of Experimentally Observed (exp) and Predicted (pred) Motional Averaging of  $^{13}\text{C}$  Chemical Shift Anisotropies in Monoclinic  $\text{C}_{70}$  Extracted from Ref 12 and MAS NMR Simulated (sim) Values in  $\text{C}_{70}\text{S}_{48}$**

carbon site	$(\delta'/\delta)_{\text{pred}}:\text{C}_{70}$	$(\delta'/\delta)_{\text{exp}}:\text{C}_{70}$	$(\delta'/\delta)_{\text{sim}}:\text{C}_{70}\text{S}_{48}$
C1	0.819	0.810	0.740
C2	0.253	0.135	-0.254
C3	-0.125	-0.210	
C4	-0.436	-0.360	-0.300
C5	-0.500	-0.385	

ments, it is not possible to determine precisely the motionally averaged chemical shift anisotropy (CSA) tensor of C2 and C3 because of NMR line overlapping.

Table 1 presents a comparison of the experimentally determined motionally averaged anisotropies  $\delta'/\delta$ , with the predictions of the simple uniaxial rotation model. These values are also compared with simulated values obtained by fitting our  $\text{C}_{70}\text{S}_{48}$  slow MAS spectrum.

$$(\delta/\delta')_{\text{pred}} \equiv (3 \cos^2 \beta - 1)/2$$

Here  $\delta = 200$  ppm (line width at 50 K), and  $\beta$  is the angle between  $\hat{n}$  and the direction normal to the plane determined by the positions of the three nearest-neighbor carbon atoms. From

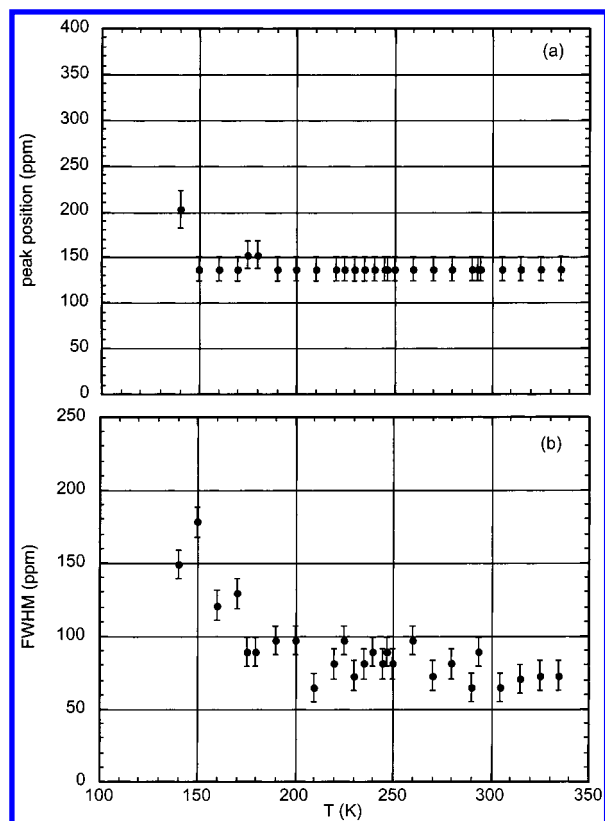


**Figure 4.** (a) <sup>13</sup>C static NMR lines position of C<sub>70</sub>S<sub>48</sub> as a function of temperature. The peak position does not change much. (b) <sup>13</sup>C full width at half-maximum as a function of temperature. A line broadening occurs below 170 K.

these results, we conclude that the C<sub>70</sub> molecules in our compound rotate uniaxially.

The study of <sup>13</sup>C static NMR spectra as a function of temperature revealed that the peak position does not change significantly with the temperature (Figure 4a) and the line widths broaden below 170 K (Figure 4b). As we study static lines, it is normal to have such a broad NMR line ( $\pm 80$  ppm) in place of the five thin MAS lines. Around 150 K, we nearly have the same line width as that observed in pure C<sub>70</sub> at 50 K (a broad powder pattern of  $\pm 200$  ppm). The broadening of the powder-pattern line shape below 150 K indicates that the rate of large-amplitude molecular reorientation has become slow with respect to the CSA width.

**3.2.2. <sup>13</sup>C Spin–Lattice Relaxation Time.** At each temperature, the <sup>13</sup>C magnetization curve for the C<sub>70</sub> line of C<sub>70</sub>S<sub>48</sub> is single exponential, as it is for pure C<sub>70</sub> above:

$$m(t) = m_0(1 - Ae^{-t/T_1})$$

with  $A \approx 1$ . This means that a single spin–lattice relaxation time exists at each temperature. In Figure 5, we see the spin–lattice relaxation rate ( $1/T_1$ ) data vs temperature and the simulated  $1/T_1$  curve based on the two activation energies (4062 and 2321 K) found by dielectric measurements. We fit the spin–lattice relaxation data with an axially symmetric CSA tensor:<sup>12</sup>

$$\frac{1}{T_1} = \frac{2}{15} \frac{\gamma^2 \mathbf{B}_0^2 S^2}{\omega} \frac{\omega \tau}{1 + \omega^2 \tau^2}$$

with a correlation time  $t$  which follows the usual Arrhenius law:

$$\tau = \tau_0 e^{E_a/T}$$

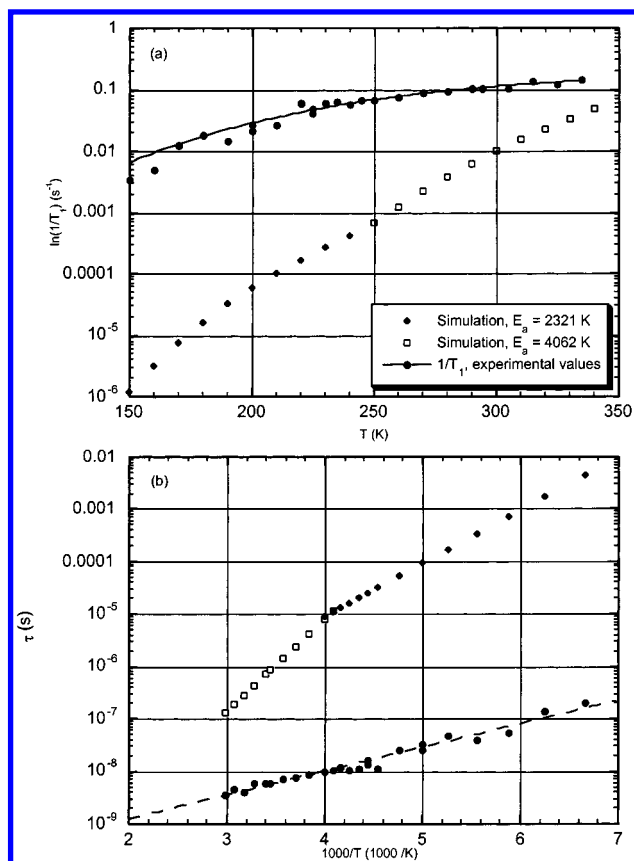


**Figure 5.** <sup>13</sup>C spin–lattice relaxation rate  $1/T_1$  of C<sub>70</sub>S<sub>48</sub> vs temperature fitted by CSA model and  $1/T_1$  simulated curve based on the dielectric activation energies 2321 and 4062 K (a). Correlation time vs  $1000/T$  extract from spin–lattice relaxation and dielectric data (b). The same symbols were used for both parts (a and b).

where  $\gamma$  is the <sup>13</sup>C magnetogyric ratio ( $67.31 \times 10^6$  rad s<sup>-1</sup> T<sup>-1</sup>),  $\mathbf{B}_0 = 7.05$  T is the static magnetic field,  $\omega = \gamma \mathbf{B}_0 = 4.75 \times 10^8$  rad s<sup>-1</sup> is the angular Larmor frequency,  $\tau$  is the rotational correlation time of the C<sub>70</sub> molecules,  $E_a$  is the activation energy, and  $S = 72$  ppm ( $5 \times 10^{-4}$  T). The  $1/T_1$  fit gives another activation energy which is 900 K (77.6 meV) and smaller than those obtained by dielectric measurements. The probable reasons for this difference will be discussed below.

As demonstrated in Figure 5, the transition seen by dielectric measurements is weak in the NMR scale. Regarding the NMR data and the fit, we observe only a slow fit divergence below 245 K.

#### 4. Discussion

In contrast to conventional spectroscopic methods, like NMR or vibrational spectroscopy, the DRS is especially sensitive to intermolecular interactions. In particular, the latter is able to monitor cooperative processes and, thus, provide a link between molecular spectroscopy or NMR, which monitors properties of individual constituents, and techniques characterizing the bulk properties of the sample (for example, X-ray diffraction). Thus, dielectric measurements and NMR are complementary methods for the study of the C<sub>70</sub>S<sub>48</sub> molecular dynamic.

Pure solid C<sub>70</sub> shows a number of phase transitions, and the sequence of phases is still unclear. Nevertheless, most studies agree that at a high temperature ( $T > 340$  K) the C<sub>70</sub> molecules undergo free rotation, whereas below this temperature, the rotation becomes anisotropic. Near room temperature (273 K  $< T < 340$  K), the rotation around the long axis of the C<sub>70</sub> molecules is dominant, and below  $\sim 273$  K, the free rotation



about the *C* axis becomes frozen in the time scale of the NMR experiments. It is interesting to compare how the insertion of sulfur rings to the structure influences the rotational properties of  $C_{70}$ . In contrast to trivial expectations, the rotation of  $C_{70}$  molecules is not hindered by sulfur, according to our NMR data, and even at room temperature, it is uniaxial like pure  $C_{70}$ . The numerous phase transitions observed for pure  $C_{70}$  have no analogues in  $C_{70}S_{48}$ . The only anomaly of the dielectric function is at 245 K. This anomaly could be attributed to a phase transition because it has a frequency-independent position. However, Differential scanning calorimetry found no anomalies at this temperature. NMR data also showed no change in the rotational properties of the  $C_{70}$  molecules around this temperature. Below we discuss some considerations on the probable nature of this anomaly.

The structure of  $C_{70}S_{48}$  was determined independently by two different groups, one at room temperature<sup>3</sup> and another at 100 K.<sup>4</sup> It is important to note that both structure solutions gave the same space group, *Amm*2. In accordance with refs 3 and 4, the structure of  $C_{70}S_{48}$  is layered. The  $C_{70}$  molecules form planes perpendicular to the *a* direction which are intercalated by a complex array of crown-shaped  $S_8$  rings. The long axes of all  $C_{70}$  molecules (the 5-fold molecular rotation axes) are pointed along the *b* axis. In accordance with the first analysis of Roth and Adelmann<sup>3</sup> at room temperature, there are two independent  $C_{70}$  molecules in the unit cell. They differ only by a 2-fold rotation around the *b* axis. Every  $C_{70}$  molecule is surrounded by 14  $S_8$  molecules, giving  $C_{70}$ -14( $S_8$ ) configurations.

In accordance with Bürgi et al.,<sup>4</sup> two  $S_8$  molecules which occupy the *a,c* mirror plane are disordered over two orientations, with population coefficients 0.8 and 0.2. However, the original analysis<sup>3</sup> does not report such a disorder. To overcome this discrepancy, we suggest that the difference between the structures in refs 3 and 4 corresponds not to a different approach to structure solving as suggested in ref 4 but to a real structural difference at low (100 K) and high (room) temperatures. We believe that the anomaly which we observe at 245 K corresponds to a change in population coefficients of the two different  $C_{70}$ -14( $S_8$ ) configurations. It is also possible to imagine this change in a reverse way, as a rotation of a part of the  $C_{70}$  molecules relative to the  $S_8$  rings. This means that the part of the  $C_{70}$  molecules which form a major  $C_{70}$ -14( $S_8$ ) configuration at low temperatures changes its orientation by a 36° rotation to give the minor configuration, and as a result, the population of both configurations are equalized.

It is necessary to underline that such a change would provide a change of the dipolar structure of  $C_{70}S_{48}$  because of the changes in the population of the two  $C_{70}$ -14( $S_8$ ) configurations. In accordance with ref 2, the  $C_{70}S_{48}$  structure contains  $C^+-S^-$  permanent dipole moments formed by nearest neighbors, so-called "electrophilic" S and "nucleophilic" C atoms with small negative and positive effective charges, respectively. Clearly, two different  $C_{70}$ -14( $S_8$ ) configurations should exhibit two different dipole moments. The sum of these dipole moments throughout the crystal lattice gives a nonzero dipole moment of the unit volume (the spontaneous polarization). Evidently, the low and high-temperature phases should have different spontaneous polarizations. The maxima of  $\epsilon'$  and  $\sigma$  at about 245 K are indicative of an anomalous response of polarization to an exciting electric field.

As for the Debye-like relaxation anomalies existing above the 245 K phase transition point (Figure 1) and below it (Figure 2), whose temperature positions depend on the frequency of the exciting electric field, we suggest that they are related to

the reorientations of the  $C^+-S^-$  dipole moments. These reorientations are consistent with a  $C_{70}$  molecule jumplike rotation around the direction of their long axis by 36° between the two states. The energy barriers between these states (configurations) are  $U^{LT} = 0.2$  and  $U^{HT} = 0.35$  eV. The attempt frequency of jumping in the low-temperature phase is about 3 orders of magnitude lower than that in the high-temperature phase. It is worth noting that the half widths of the loss peaks both below and above 245 K are somewhat larger than those of a standard Debye relaxation. Clearly, it is related to a particular distribution of relaxation times.

The anomaly of dielectric function has no clear counterpart in the NMR data. According to NMR, the  $C_{70}$  molecules rotate uniaxially at room temperature, but as it can be seen from Figure 4, below 170 K, this rotation begin to freeze, and at 150 K, the rotation is frozen in the NMR scale. Furthermore, relaxation times found by NMR are of the same order but less than those obtained by the dielectric function study. Thus, the one method which was used does not clearly confirm rotational changes found by the other one. Dielectric function temperature dependence does not show any anomalies around 170 K, where the NMR registered the freezing of the rotational freedom of the  $C_{70}$  molecules, and the NMR does not shows any features around 245 K, where the dielectric function shows a sharp anomaly. In some cases, the temperature for anomalies of the same microscopic nature found by different methods may show several tens of degrees difference if it is influenced by the time scale of each method. Such a situation was observed, for example, in the  $C_{60}$  "glassy" transition, where the temperature of this transition was found in the range  $80 < T < 182$  K, depending on the used method.<sup>16</sup> The higher frequency method registered an anomaly at higher temperatures, but in our studies, the reverse situation was observed, and the possibility of the "glassy" transition around 245 K must be ruled out.

In principle, as we noted above, DRS and NMR are complementary methods, and they do not have to show the same results. NMR studies only the carbon atoms, whereas the dielectric function includes cooperative effects from the whole structure and particularly  $C_{70}$ - $S_8$  configurations. With this fact taken into account, the difference in relaxation times seems to be reasonable. The change in the dipole moment at 245 K is possible, in principle, without significant changes in the rotational state of the  $C_{70}$  molecules. Also it needs to be noted that the frequency used in the NMR experiments (75.5 MHz) is much higher than the frequencies applied for the dielectric function studies (20 Hz to 1 MHz). This fact should not influence the frequency-independent anomaly at 240 K but may be a reason for why DRS does not recognize the freezing of the  $C_{70}$  rotation below 170 K.

In conclusion, the anomaly found by our dielectric function study at 245 K is not confirmed by NMR. With concern for the nature of this anomaly, it may be suggested that there is a change in the rotational state of the  $C_{70}$  molecules rather than a phase transition. Our assumptions allow us to suggest that the two  $C_{70}$ -14( $S_8$ ) configurations have different population coefficients at room and at low temperatures, with a jumplike change between them at 245 K.

**Acknowledgment.** The Swedish Natural Science Research Council (NFR) is acknowledged for financial support. F.M. and A.-S.G. were supported by the BNB (Banque Nationale de Belgique) and acknowledge the help of P. Lentz for MAS simulation.

## References and Notes

- (1) Roth, G.; Adelman, P. *Appl. Phys. A* **1993**, 56, 169.
- (2) Roth, G.; Adelman, P.; Knitter, R. *Mater. Lett.* **1993**, 16, 357.
- (3) Roth, G.; Adelman, P. *J. Phys. I* **1992**, 2, 1541.
- (4) Bürgi, H. B.; Venugopalan, P.; Schwarzenbach, D.; Diederich, F.; Thilgen, C. *Helv. Chim. Acta* **1993**, 76, 2155.
- (5) Talyzin, A. V.; Tergenius, L.-E.; Jansson, U. *J. Cryst. Growth* **2000**, 213, 63.
- (6) Michel, R. H.; Kappes, M. M.; Roth, G.; Adelman, P. *Angew. Chem., Int. Ed. Engl.* **1994**, 33, 1651.
- (7) Semkin, V. N.; Drichko, N. V.; Talyzin, A. V.; Graja, A.; Krol, S.; Konarev, D. N.; Lyubovskaya, R. N. *Synth. Met.* **1998**, 93, 207.
- (8) Talyzin, A. V.; Jansson, U. *Thin Solid Films* **1999**, 350, 113.
- (9) Talyzin, A. V.; Ratnikov, V. V.; Syrnikov, P. P. *Phys. Solid State* **1996**, 7, 1531.
- (10) Sherman, A. B.; Talyzin, A. V.; Elgholabzouri, M.; Lemanov, V. V.; Jansson, U.; Lunkenheimer, P.; Brand, R.; Loidl, A. *Mol. Cryst. Liq. Cryst. Sci. Technol., Sect. C* **2000**, 13, 269.
- (11) Grell, A.-S.; Masin, F.; Céolin, R.; Gardette, M.-F.; Szwarc, H. *Phys. Rev. B* **2000**, 62, 3722.
- (12) Tycko, R.; Dabbagh, G.; Vaughan, G. B. M.; Heiney, P. A.; Strongin, R. M.; Cichy, M. A.; Smith, A. B., III. *J. Chem. Phys.* **1993**, 99 (10), 7554.
- (13) Taylor, R.; Hare, J. P.; Abdul-Sada, A. K.; Kroto, H. W. *J. Chem. Soc., Chem. Commun.* **1990**, 1423.
- (14) Masin, F.; Grell, A.-S.; Messari, I.; Gusman, G. *Solid State Commun.* **1998**, 106, 59.
- (15) Tekely, P.; et al. *Solid State Commun.* **1998**, 106, 391.
- (16) Dresselhaus, M. S.; Dresselhaus, G.; Eklund, P. C. *Science of Fullerenes and Carbon Nanotubes*; Academic Press: New York, 1996; pp 190–192.